RESEARCH PAPER

Novel Observer-Based Input-Constrained Control of Nonlinear Second-Order Systems with Stability Analysis: Experiment on Lever Arm

Faezeh Pak[1] · Mehdi Mirzaei[1] · Sadra Rafatnia[1] · Sasan Salmani Pour Avval[1]

Abstract

In this survey, the stability of input-constrained control for a widely used class of second-order systems is investigated. A continuous prediction-based approach is utilized to calculate the limited current control input by minimizing the next tracking error of nonlinear second-order system. The Karush–Kuhn–Tucker theorem is used to analytically solve the resulting constrained optimization problem. The constrained stability is analyzed by equating the constrained solution with the solution obtained from an optimal controller with time-varying weight on the control input. The proposed constrained controller adapts itself to real conditions by using information about the perturbations obtained from an extended state observer (ESO). Simulation studies for a lever arm indicates that the constrained controller presented in the closed form is much faster than the common nonlinear model predictive control method which requires an online dynamic optimization at each sampling time. Accordingly, experimental implementation of the proposed controller is conducted on a fabricated platform consisting of a lever arm. The results show that the proposed constrained controller can successfully track different time-varying positions for the arm by admissible torques generated by a DC motor. The comparative results with an adaptive backstepping controller indicate higher performance for the proposed ESO-based controller in compensating for the perturbations and external disturbance.

Keywords Second-order system · Constrained stability · Optimal control · Lever arm · Uncertainty observer

1 Introduction

Nonlinear second-order systems include a widely used mechanical and electromechanical systems such as robot manipulator, spacecraft, underwater vehicle, wind turbine and vibrating systems (Colombo et al. 2020; Jiang et al. 2022; He et al. 2022; Nguyen et al. 2020). The variety of applications has motivated many researchers in the last decades to control the second order systems by different strategies (Li et al. 2021; Jimenez-Rodriguez et al. 2019; Bartolini et al. 1997; Li et al. 2022). Bartolini et al. (1997) solved the tracking problem of nonlinear second-order systems by classical minimum-time optimal control method. A tracking control scheme using reinforcement learning is proposed to steer both position and velocity of a class of second-order systems (Li et al. 2022). A multi-agent second-order system is controlled by a neural network-based controller which can ensure that the tracking errors between the following agent and leader will converge to a narrow neighborhood of zero (Wen et al. 2015). A velocity observer-based feedback controller is developed for second-order systems with the application to a robot (Homayounzade and Keshmiri 2011). A finite-time sliding mode control that employs a disturbance observer is presented for second-order systems (Miranda-Colorado 2019).

Most research conducted on the control of second-order systems tried to solve the tracking problem without attention to the practical limitations (Ghiasi et al. 2010). In this respect, the limitation on the control input plays a significant role in finding the feasible control signal. This restriction results from the limited capacity of actuators like DC motors, which can just generate a finite amount of torque. Neglecting the input constraint in designing the controllers has a negative effect on the closed-loop system performance. To address this problem, various methods

✉ Mehdi Mirzaei
  mirzaei@sut.ac.ir

[1] Faculty of Mechanical Engineering, Sahand University of Technology, Tabriz 513351996, Iran

have been employed for input-constrained control by taking into consideration one or multiple requirements like stability, practical implementations, simplicity in computations, robustness, optimality and generality. One solution incorporates static or dynamic nonlinear models to represent the saturation within the system model (Gui et al. 2015). Another solution is to use anti-windup schemes jointed to the main controllers to counteract the impact of input saturation within the control systems (Tsai et al. 2011). Proportional derivative controller integrated with a dynamic compensation (Su and Swevers 2014) and intelligent methods plus Barrier Lyapunov functions (Ma and Huang 2020) are also proposed as alternative solutions for the saturated control problems. Ding and Zheng (2016) designed terminal sliding mode control for nonlinear second-order systems with input saturation. In all of the reviewed methods, optimization is not the primary procedure to solve the constraint issue for finding the control laws. Meanwhile, the stability and universality of the previously mentioned approaches might still lack clarity.

The optimality of solutions for constrained nonlinear systems can be achieved through dynamic programming or calculus of variation as the classical optimal control methods (Kirk 2004). Because of high computations of these methods, some approximation methods based on piecewise functions (Loxton et al. 2009) Haar functions (Marzban and Razzaghi 2010), adaptive dynamic programming (ADP) (Liu et al. 2013), hybrid functions (Mashayekhi et al. 2012) and adaptive neural network approaches (Li et al. 2017) are applied to approximate the control input. Alternatively, modern optimal methods such as model predictive control (MPC) have been introduced to find the constrained control inputs at each sampling time by solving an optimization problem online (Silva et al. 2019). Although MPC strategies are suitable for linear systems, extending them to nonlinear systems introduces new challenges. It is difficult or impossible to find analytical solution for the optimization problem in the nonlinear problems. The numerical solutions also involve high computations, making them unsuitable for online implementations. Importantly, the stability analysis of NMPC methods in the presence of constraints requires further research.

In the current paper, in order to overcome the time-consuming problem in the optimization-based nonlinear methods reviewed above, a control strategy is proposed for the second-order systems based on a continuous predictive approach. This approach, unlike the conventional discrete predictive control, leads to the closed form control laws with no need to the optimization process at each sampling time. The proposed approach leads to feedback linearization-like method when the constraints are dropped and the uncertainties of the system are ignored (Moradi Nerbin

et al. 2017; Lu 1995; Abdi et al. 2018; Rafatnia and Mirzaei 2022). For the uncertain systems, the tracking error is decreased by selecting small values for the prediction time as a free parameter of the controller (Mirzaeinejad et al. 2016; Rafatnia and Mirzaei 2022). In the present study, the constrained version of the continuous predictive approach is developed by minimizing the expanded performance index in the presence of input constraints. The Karush–Kuhn–Tucker (KKT) theorem is used to analytically solve the resultant constrained optimization problem. How to solve the KKT conditions in a straight-forward manner for the second-order system is demonstrated in this paper. Importantly, the boundedness of the tracking error and its derivative for the second order system is provided by equating the constrained solution with the solution obtained from an optimal controller with a time-varying weight on the control input.

It is important to note that the constrained controller, developed for the second order system, requires a precise mathematical model to reach the desired performance. However, there are various sources of perturbations, including un-modelled dynamics, uncertain parameters and external disturbances, deteriorating the performance of model-based control system (Razmjooei et al. 2022). Different control methods have been suggested by the researchers to deal with uncertainties and disturbances. Among these studies, two commonly used techniques can be distinguished as robust and adaptive control methods (Yi and Zhai 2019; Hu et al. 2022; Cruz-Ortiz et al. 2022). In the paper, an extended state observer (ESO) is utilized to enhance the nominal model considered for the second-order systems (Xiong et al. 2015). The ESO has been applied in various applications like robot control (Yue et al. 2014) and flight control (Li et al. 2014). The paper integrates the constrained controller with the ESO to develop an adaptive constrained controller. The resultant control system can continuously adapt itself by using the observer information about the perturbations without increasing the order of main system.

For a case study, the position control problem of a lever arm as a second-order system is selected to examine the proposed controller. In the simulation study, the NMPC has been used as a comparative method to show the performance and applicability of the proposed constrained controller. For experimental implementation, a platform for lever arm control is fabricated to verify the proposed controller under various maneuvers of trajectory tracking. An experimental assessment is conducted to compare the efficiency of a constrained controller with and without an observer, considering different trajectories. Also, an adaptive backstepping controller is implemented to be compared with the ESO-based constrained controller in the presence of perturbations.

The paper is organized as follows: In Sect. 2, the problem formulation in a general form is presented and the design and analysis of the control system are proposed. In this section, the constrained controller is firstly design, supposing that the perturbation term in the model of the second order system is known. Then, the ESO algorithm is presented to estimate the perturbation term. In Sect. 3, the results of the proposed control method are presented for a lever arm under computer simulations and experimental implementations. Finally, Sect. 4 gives the conclusion.

2 Control Problem Definition

The aim of this study is controlling a widely used class of second-order systems in the presence of input constraint caused by limited capacity of actuators, and perturbations caused by model uncertainties and external disturbances. The dynamic of the many practical systems like Euler–Lagrange systems is derived as Jiang et al. (2022); Li et al. (2022); Miranda-Colorado (2019)

$$\ddot{x} = f(x, \dot{x}) + bu + d. \tag{1}$$

where $x \in R$ is the generalized position and $\dot{x} \in R$ is the generalized velocity. $u \in R$ is the control input that is manipulated to control the generalized position with the bounded generalized velocity. In addition, d is the unexpected external disturbance, respectively. Considering $\eta(x, \dot{x}, d) = f(x, \dot{x}) + d$ as the perturbation term, and $x_1 = x$ and $x_2 = \dot{x}$ as the states of the system, the state-space form of (1) is represented as follows:

$$\begin{cases} \dot{x}_1 = x_2, \\ \dot{x}_2 = \eta(x, \dot{x}, d) + bu, \\ y = x_1. \end{cases} \tag{2}$$

Assumption: It is supposed that $\eta(x, \dot{x}, d)$ is a bounded function, and also $b \neq 0$ is a constant (Li et al. 2021, 2022; Miranda-Colorado 2019).

There is often a constraint on the control input of the system due to the limited capacity of the onboard actuators. In this study, the admissible range for the control input is considered as follows

$$u = \{u \in R \mid U_{\min} \le u \le U_{\min}\}. \tag{3}$$

The other challenge with the state space Eq. (2) is the perturbations existing in $\eta(x, \dot{x}, d)$, making the system model improper for the constrained controller design. One strategy to deal with this challenge is using the estimation methods. In this paper, the ESO is used to upgrade the nominal model toward the actual system. In this high-gain observer, $y = x_1$ is considered as the system output.

The structure of the ESO-based constrained control system is shown in Fig. 1. By using the information of measurable output, the ESO aims to estimate the uncertainty term $\eta(x, \dot{x}, d)$ to minimize the difference between the nominal model and the actual model. Consequently, assuming an reliable dynamic model for the system, the constrained controller is initially designed based on the model outlined in (2). Subsequently, the supervisor updates the control law by utilizing information received from the observer. Therefore, the ESO-based constrained controller adapts itself with reality to track the desired trajectories.

2.1 Constrained Controller Design

In this section, the control law is developed using an optimization approach by assuming that the perturbation term $\eta(x, \dot{x}, d)$ is known. In this approach, the quadratic point-wise performance index defined as a weighted combination of the current control signal and the next tracking error is considered to be minimized as Mirzaeinejad and Mirzaei (2011); Jafari et al. (2015)

$$J = \frac{1}{2}[x_1(t+h) - x_{1d}(t+h)]^2 + \frac{1}{2}wu^2, \tag{4}$$

in which h is the prediction time, and x_{1d} is the desired output. The weighting factor w shows the relative importance of control energy and tracking accuracy. By increasing w, the control input is reduced at the cost of decreasing the tracking accuracy. The term $x_1(t+h)$ is approximated by the qth-order Taylor series expansion at the present time t

$$x_1(t+h) = x_1(t) + h\dot{x}_1(t) + \frac{h^2}{2!}\ddot{x}_1(t) + ... + \frac{h^q}{q!}x_1^{(q)}(t). \tag{5}$$

For the control algorithm, the order of Taylor series expansion in (5) is limited to the relative degree of the expanded control variable (Moradi Nerbin et al. 2017; Lu 1995). The second-order system has the relative degree, $\rho = 2$, for x_1 because the control input u appears explicitly in the second derivative of x_1 for the first time according to the system model defined by (1) and (2).
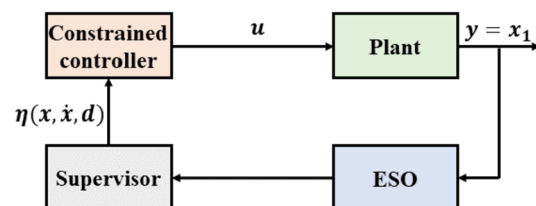

Fig. 1 Block diagram of the ESO-based controller

Remark 1 By limiting the expansion order equal to the relative degree of the control variable, the control input is supposed to be constant in the predictive interval between t and $t + h$. This means zero control order and is sufficient for control variables with low relative degrees. Increasing the control order causes complexity in the calculation of the control input (Mirzaeinejad et al. 2016; Malekshahi and Mirzaei 2012).

By considering the perturbation term η as a known factor, in the following, the output and its desired value is expanded by the second-order Taylor series:

$$x_1(t + h) = x_1(t) + hx_2(t) + \frac{h^2}{2}(\eta + bu). \tag{6}$$

$$x_{1d}(t + h) = x_{1d}(t) + h\dot{x}_{1d}(t) + \frac{h^2}{2}\ddot{x}_{1d}(t). \tag{7}$$

By substituting Eqs. (6) and (7) into (4), the performance index is rewritten in terms of current states and variables as

$$J = \frac{1}{2}\left[(x_1 - x_{1d}) + h(x_2 - \dot{x}_{1d}) + \frac{h^2}{2}(\eta + bu - \ddot{x}_{1d})\right]^2 + \frac{1}{2}wu^2. \tag{8}$$

By using the system dynamics described by Eq. (1), the performance index (8) is written in terms of the system states and input in the present time. Accordingly, the optimal control law for a second-order system is obtained by applying the subsequent necessary condition for optimality, which relates to the quadratic performance index (8):

$$\frac{\partial J}{\partial u} = 0, \tag{9}$$

which leads to

$$u = -\frac{2\kappa}{bh^2}\left[e_1 + h(x_2 - \dot{x}_{1d}) + \frac{h^2}{2}(\eta - \ddot{x}_{1d})\right], \tag{10}$$

where $e(t) = x_1 - x_{1d}$, and the reduction factor, which incorporates the control weighting factor, is defined as follows:

$$\kappa = \frac{1}{1 + 4h^{-4}b^{-2}w}, \tag{11}$$

where $0 \leq \kappa \leq 1$ for $w \geq 0$. By increasing the weighting factor w, the reduction factor κ is reduced to limit the control input. When $w = 0$, then $\kappa = 1$. In this case, the control input with no intentional reduction is given as

$$u = -\frac{2}{bh^2}\left[e_1 + h(x_2 - \dot{x}_{1d}) + \frac{h^2}{2}(\eta - \ddot{x}_{1d})\right]. \tag{12}$$

Using the control law (12) in the model (2), the closed loop dynamics is achieved as

$$\dot{x}_2 = f - \frac{2}{h^2}\left[e_1 + h(x_2 - \dot{x}_{1d}) + \frac{h^2}{2}(\eta - \ddot{x}_{1d})\right], \tag{13}$$

that leads to the following error dynamics:

$$\ddot{e}_1 + \frac{2}{h}\dot{e}_1 + \frac{2}{h^2}e_1 = 0. \tag{14}$$

Remark 2 By deriving the control laws (10) and (12) in the closed forms, the prediction time h is considered as a free parameter of the control law, not a step size of integration. This free parameter should be adjusted to achieve a desired behaviour for the closed loop system. Since the parameter h is selected positive, the linear error dynamics (14) is exponentially stable. This result indicates that the truncation error in Taylor series expansion with the order limited to the relative degree does not influence the control performance as mentioned in Remark 1. The parameter h also influences the time constant of the closed-loop system (14). The poles of the closed loop system (14) are determined as $\frac{-1}{h}(1 + j)$. It is seen that, h affects the place of poles and consequently the system response. Faster responses are achieved with smaller values of h.

For the constrained control problem, the performance index (8) is minimized subject to the satisfaction of constraints (3). One strategy for restricting the control input within a specified range is the increasing of the weighting factor w in the control law (10). For a constant value of w, the control input is decreased during the process at the cost of increased tracking errors at all times even when the control input is within the range.

As an alternative optimal approach, the constrained controller is developed in which the input constraint is considered in finding the control law. To achieve this aim, the expanded performance index (8) with $w = 0$ has to be minimized in the presence of the input constraints (3). As a result, the following constrained optimization problem needs to be solved to determine the optimal control law:

$$\begin{aligned} \text{minimize} \quad & J(u(t),\ x(t), h, w = 0) \\ \text{subject to} \quad & U_{\min} \leq u \leq U_{\max}. \end{aligned} \tag{15}$$

The analytical solution to the constrained optimization problem (15) is achieved by applying the KKT theorem. Accordingly, the input constraint with upper and lower bounds is written as two constraints in the following standard form:

$$p_1(u) = u - U_{\max},$$
$$p_2(u) = -u + U_{\min}. \tag{16}$$

Then, the KKT conditions for optimality can be expressed as Rao (2019):

$$\frac{\partial J}{\partial u} + \sum_{i=0}^{2} \lambda_i \frac{\partial p_i}{\partial u} = 0, \ i = 1, 2 \tag{17}$$

$$\lambda_i p_i = 0 \quad i = 1, 2 \tag{18}$$

$$p_i \leq 0 \qquad i = 1, 2 \tag{19}$$

$$\lambda_i \geq 0 \qquad i = 1, 2 \tag{20}$$

where λ_1 and λ_2 denote Lagrange multipliers.

Theorem 1 *For the affine system* (1)–(2) *having single input, $u \in R$, with upper and lower constraints, the constrained solution leads to the simple saturation of the unconstrained control.*

Proof The KKT conditions (17) to (20) include some equalities and inequalities that are solved simultaneously by considering activity or inactivity of constraints. According to (18), the inactive constraints imply $p_i \leq 0$ and $\lambda_i = 0$, while for active constraints $\lambda_i \neq 0$ and $p_i = 0$. In the mentioned problem, both constraints cannot be active simultaneously. Therefore, when one of the constraints becomes active, its Lagrange multiplier takes a non-zero value, and the control input is readily determined using the constraint equation with equality sign ($p_i = 0$), as specified in (18). Accordingly, the non-zero Lagrange multiplier corresponding to inactive constraint can be calculated by solving Eq. (17). During instances when none of the constraints are active, all Lagrange multipliers are zero, resulting in an optimal solution without constraints. Consequently, the constrained control law for the second-order system is derived as follows:

$$u_{\text{cons}} = \begin{cases} U_{\max} & \text{if} \quad p_1 \geq 0, \ p_2 < 0 \\ u_{\text{unc}} & \text{if} \quad p_1 \leq 0, \ p_2 \leq 0 \\ U_{\min} & \text{if} \quad p_1 < 0, \ p_2 \geq 0 \end{cases} \tag{21}$$

where u_{unc} is the unconstrained control law presented in (12). Note that for the second-order system (1)–(2), the form of performance index (4) or (8) is parabolic having a single minimum. Therefore, a feasible solution with bounded Lagrange multipliers exist for KKT conditions.

According to the error dynamics (14), the unconstrained control system with $w = 0$ is exponentially stable. On the other hand, from Theorem 1, the optimal constrained solution given in (21) is a simple saturation of the unconstrained optimal control law with $w = 0$. This solution can be achieved, equivalently, by online regulating of the weighting factor w in the control law (10). In other

words, the saturated control input (21) can be achieved by tuning the reduction factor in the unconstrained control law (10). Consequently, the coefficient κ is occasionally reduced from 1 to avoid surpassing the allowable input value. The coefficient κ corresponding to the maximum input is derived from (10) as follows:

$$\kappa = -u_{\text{cons}} \frac{bh^2}{2} \left[e_1 + h(x_2 - \dot{x}_{1d}) + \frac{h^2}{2} (\eta - \ddot{x}_{1d}) \right]^{-1}. \tag{22}$$

For other times when the control input is within the admissible range, the coefficient κ will be equal to 1, that means no reduction on the control input.

In the following, two different approaches are conducted to show the boundedness of tracking error under the control input (21) when the control input is weighted with a time-varying variable to decrease κ. Equivalently, the boundedness of saturation solution is provided.

Theorem 2 *The tracking error of generalized position and its derivative in the closed-loop system under the control law* (10) *are uniformly bounded for any $0 \leq \kappa \leq 1$.*

Proof The closed loop dynamics in terms of κ is derived by applying Eq. (10) into Eq. (1) as follows:

$$\ddot{e}_1 + \frac{2\kappa}{h} \dot{e}_1 + \frac{2\kappa}{h^2} e_1 = (1 - \kappa)(\eta - \ddot{x}_{1d}). \tag{23}$$

The right hand-side of Eq. (23) is created due to the limiting of the control input that causes some tracking errors. For $\kappa = 1$, the closed loop dynamics (23) is changed to Eq. (14) indicating no constraint case. Assuming that the function η in (2) is bounded and considering $|\eta - \ddot{x}_{1d}| < \Gamma$, Eq. (23) can be written as

$$\ddot{e}_1(t) + \frac{2\kappa}{h} \dot{e}_1 + \frac{2\kappa}{h^2} e_1 < (1 - \kappa)\Gamma. \tag{24}$$

By using the solution of the second-order differential equation, followed by the application of the comparison lemma (Khalil 2001), it is established that

$$e_1 \leq A e^{\frac{-\kappa}{h} t} \left(\sin \frac{\sqrt{\kappa(2 - \kappa)}}{h} t + \phi \right) + \frac{(1 - \kappa)\Gamma h^2}{2\kappa}. \tag{25}$$

The positive value of h indicates that

$$\lim_{t \to \infty} e_1(t) = \frac{(1 - \kappa)\Gamma h^2}{2\kappa}. \tag{26}$$

Substituting Eq. (11) in (26) leads to

$$\lim_{t \to \infty} e_1(t) = \frac{2\Gamma w}{h^2 b^2}. \tag{27}$$

From equation (27), it can be deduced that, for any specified $\epsilon > 0$, selecting the prediction time h as $h^2 > \frac{2w\Gamma}{b^2\epsilon}$

guarantees the convergence of e_1 towards the following compact set:

$$|e_1| < \epsilon. \tag{28}$$

To assess the boundedness of $\dot{e}_1(t)$ for the second-order system, one can examine a potential candidate for the Lyapunov function in the form of

$$V = \frac{\kappa}{h^2} e_1^2 + \frac{1}{2} \dot{e}_1^2 > 0. \tag{29}$$

The first time derivative of V gives

$$\dot{V} = \frac{\dot{\kappa}}{h^2} e_1^2 + \frac{2\kappa}{h^2} e_1 \dot{e}_1 + \dot{e}_1 \ddot{e}_1. \tag{30}$$

When the control input reaches the constraint, κ is equivalently reduced from 1 to decrease the control input, so $\dot{\kappa}$ in Eq. (30) becomes negative until the saturation is removed and the system returns to the unconstrained solution. For the un-constrained solution, $\kappa = 1$ and $\dot{\kappa} = 0$. Therefore, Eq. (30) is simplified to

$$\dot{V} = -\frac{2}{h} \dot{e}_1^2 < 0, \tag{31}$$

that indicates the asymptotic stability of closed loop system. For the saturated times, considering a negative value for $\dot{\kappa}$ and replacing Eq. (23) into (30) gives

$$\dot{V} = \dot{e}_1 ((1 - \kappa)(\eta - \ddot{x}_{1d})) - \left[\frac{|\dot{\kappa}|}{h^2} e_1^2 + \frac{2\kappa}{h} \dot{e}_1^2 \right]. \tag{32}$$

Considering the upper bound for $|(\eta - \ddot{x}_{1d})| < \Gamma$, gives

$$\dot{V} \le |\dot{e}_1|(1 - \kappa)\Gamma - \left[\frac{|\dot{\kappa}|}{h^2} e_1^2 + \frac{2\kappa}{h} \dot{e}_1^2 \right] \le |\dot{e}_1|(1 - \kappa)\Gamma - \frac{2\kappa}{h} \dot{e}_1^2. \tag{33}$$

Further investigation on the inequality (33) is done by applying the inequality $\alpha\beta \le n\alpha^2 + \frac{\beta^2}{4n}$ for any real α, β and $n > 0$. By considering $n = \frac{\kappa}{h} > 0$

$$\dot{V} \le \frac{\kappa}{h} \dot{e}_1^2 + \frac{h\Gamma^2(1 - \kappa^2)}{4\kappa} - \frac{2\kappa}{h} \dot{e}_1^2, \tag{34}$$

$$\dot{V} \le \frac{h\Gamma^2(1 - \kappa)^2}{4\kappa} - \frac{\kappa}{h} \dot{e}_1^2. \tag{35}$$

Using (28) and (29), the inequality (35) is rewritten as

$$\dot{V} \le -\frac{2\kappa}{h} V + \frac{2\kappa^2}{h^3} \epsilon^2 + \frac{h\Gamma^2(1 - \kappa)^2}{4\kappa}. \tag{36}$$

By taking $\frac{2\kappa^2}{h^3} |\epsilon|^2 + \frac{h\Gamma^2(1-\kappa)^2}{4\kappa} = N$, the inequality (36) is written as

$$\dot{V} \le -\frac{2\kappa}{h} V + N. \tag{37}$$

Applying the comparison lemma, the solution of the first-order differential equation results in:

$$V(t) \le \left(V(0) - \frac{hN}{2\kappa} \right) e^{\frac{-2\kappa}{h} t} + \frac{hN}{2\kappa}. \tag{38}$$

Due to the positive values of κ and h, the Lyapunov function remains bounded as can be observed

$$\lim_{t \to \infty} V(t) = \frac{hN}{2\kappa}. \tag{39}$$

The boundedness of the Lyapunov function (29), coupled with the convergence of the error e_1 within a compact set as indicated by (28) result the boundedness of $\dot{e}_1$.

Remark 3 As deduced from Theorem 2, it is imperative to avoid selecting an overly small prediction time h to ensure the system's tracking error remains within acceptable bounds under input constraints. On the other hand, the smaller value for h leads to the faster response of the systems as indicated in Remark 2. Therefore, a reasonable value for the prediction time should be selected. This issue will be investigated in the results section.

2.2 Design of ESO

In this section, the ESO algorithm is utilized to estimate the perturbation term $\eta(x, \dot{x}, d)$ for using in the constrained control law developed in the previous section. By defining the perturbation term as an extera state $x_3 = \eta(x, \dot{x}, d)$, the augmented state-space model of the system can be rewritten as

$$\begin{cases} \dot{x}_1 = x_2, \\ \dot{x}_2 = x_3 + bu, \\ \dot{x}_3 = \Upsilon(t), \\ y = x_1 \end{cases} \tag{40}$$

The equations of ESO are presented as

$$\begin{cases} \dot{\hat{x}}_1 = \hat{x}_2 - \Omega_1(\hat{x}_1 - y) \\ \dot{\hat{x}}_2 = \hat{x}_3 - \Omega_2(\hat{x}_1 - y), \\ \dot{\hat{x}}_3 = -\Omega_3(\hat{x}_1 - y), \end{cases} \tag{41}$$

in which $\Omega_{i \ (i=1,2,3)}$ represent the observer gains. With the appropriate selection of gains, the observer provides a good estimate for the system states, encompassing the additional state x_3. The error dynamics is derived by subtracting (41) from (40) as

$$\begin{cases} \dot{\tilde{e}}_1 = \tilde{e}_2 - \Omega_1 \tilde{e}_1, \\ \dot{\tilde{e}}_2 = \tilde{e}_3 - \Omega_2 \tilde{e}_1, \\ \dot{\tilde{e}}_3 = -\Omega_3 \tilde{e}_1 + \Upsilon(t), \end{cases} \tag{42}$$

in which $\tilde{e}_i = \hat{x}_i - x_i \ (i = 1, 2, 3)$ represents the error of estimation. According to Eq. (42), the error dynamics is linear. Therefore, by selecting appropriate gains, the observer stability is assured, assuming that $\Upsilon(t) = \dot{\eta}$

remains bounded. The following theorem gives a scheme for selecting the gains $\Omega_{i\ (i=1,2,3)}$ to produce the desired response.

Theorem 3 *By selecting* $\Omega_1 = 3/\epsilon$, $\Omega_2 = 3/\epsilon^2$ *and* $\Omega_3 = 1/\epsilon^3$, *in which* $\epsilon > 0$ *is an adjustable parameter, the estimation error dynamics described by (42) remains bounded under the condition of bounded* $\Upsilon(t)$.

Proof By selecting $\Omega_1 = 3/\epsilon$, $\Omega_2 = 3/\epsilon^2$ and $\Omega_3 = 1/\epsilon^3$ in (42), the resulting dynamics can be expressed as

$$\begin{bmatrix} \dot{\tilde{e}}_1 \\ \dot{\tilde{e}}_2 \\ \dot{\tilde{e}}_3 \end{bmatrix} = \Psi \begin{bmatrix} \tilde{e}_1 \\ \tilde{e}_2 \\ \tilde{e}_3 \end{bmatrix} - G\Upsilon(t), \tag{43}$$

where

$$\Psi = \begin{bmatrix} -3/\epsilon & 1 & 0 \\ -3/\epsilon^2 & 0 & 1 \\ -1/\epsilon^3 & 0 & 0 \end{bmatrix}$$

and $G = \begin{bmatrix} 0 \\ 0 \\ 1 \end{bmatrix}$. The eigenvalues of Ψ are found as $\lambda_i = -1/\epsilon$ $(i = 1, 2, 3)$. Consequently, the matrix Ψ will be Hurwitz for a given positive ϵ, ensuring the bounded-input bounded output (BIBO) stability for the error dynamics. Solving (43) yields

$$\tilde{e}(t) = e^{Et}\tilde{e}(0) + \int_0^t e^{E(t-\tau)} G\Upsilon(\tau)d\tau, \tag{44}$$

where $\tilde{e} = [\tilde{e}_1 \ \tilde{e}_2 \ \tilde{e}_3]^T$. Since ϵ is a positive value

$$\lim_{t\to\infty} \tilde{e}(t) = \int_0^t e^{E(t-\tau)} G\Upsilon(\tau)d\tau. \tag{45}$$

Based on Eq. (45), for any given $\epsilon > 0$ and under the assumption of bounded $\Upsilon(u)$, the estimation error converges to a compact set Chen (1984).

Remark 4 The positioning of eigenvalues and the convergence speed of the ESO as a high-gain observer, are impacted by the adjustable parameter ϵ. Any decrease in the value of ϵ leads to a fast response for the observer. However, decreasing the adjustable parameter ϵ increases the sensitivity to modeling errors and measurement noise, potentially resulting in increased estimation errors. Moreover, there is a risk of numerical errors during the solution of the set of differential equations at each sampling time for smaller values of ϵ.

3 Case Study (A Lever Arm)

According to Fig. 2, a lever arm consisting of a massless arm with two lumped masses at the end-points is examined as a case study for the second-order system.

In this structure, the kinematic and potential energies are obtained as follows:

$$T = \frac{1}{2}I_o\dot{\theta}^2, \tag{46}$$

$$V_g = (m_1r_1 - m_2r_2)g\sin\theta. \tag{47}$$

Here, I_o represents the moment of inertia, m_1 and m_2 are the lumped masses located at the end points of the arm, and θ represents the angular displacement of the arm. The governing equation for the lever arm using the Lagrange method is given as

$$\frac{d}{dt}\left(\frac{\partial T}{\partial \dot{\theta}}\right) - \frac{\partial T}{\partial \theta} + \frac{\partial V_g}{\partial \theta} = \tau, \tag{48}$$

which leads to

$$I_o\ddot{\theta} + G(\theta) = \tau, \tag{49}$$

where $I_o = m_1r_1^2 + m_2r_2^2$ is the lever arm inertia and $G = (m_1gr_1 - m_2gr_2)\cos\theta$ denotes the gravity term. τ represents the torque of motor. By defining $\theta = x_1$, $\dot{\theta} = x_2$, the state-space model of the lever arm is formulated as

$$\begin{cases} \dot{x}_1 = x_2, \\ \dot{x}_2 = f(x) + a\tau, \end{cases} \tag{50}$$

where

$$f(x) = -I_o^{-1}G, \ a = I_o^{-1}. \tag{51}$$

3.1 Simulation Results

In the simulation study, the dynamic model of the lever arm system is assumed to be accurate. Therefore, the
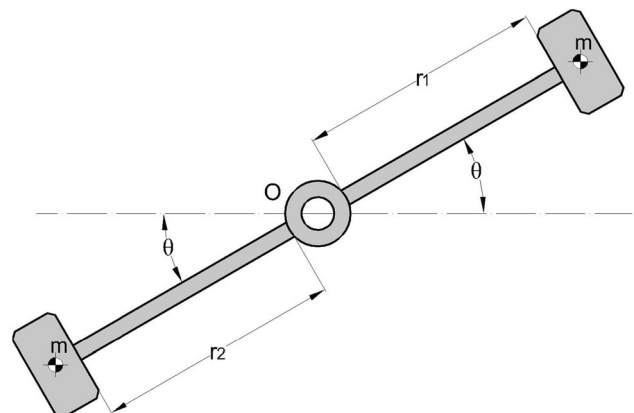

Fig. 2 The schematic of the lever arm

constrained controller is examined without the ESO observer. The parameters of the lever arm are taken as $m_1 = 0.5$ (kg), $m_2 = 0.6$ (kg), $r_1 = 0.14$ (m), $r_2 = 0.15$ (m). Also, the admissible range for the control input is considered as $-0.98 \leq \tau \leq 0.98$ (N m). Three distinct prediction times, including $h = 0.05$, $h = 0.2$, and $h = 0.4$, are examined for the proposed control system.

At first, the outcomes of the unconstrained control strategy for three distinct prediction times are illustrated in Fig. 3. Note that, the input constraint is dropped in these results. As mentioned before, the unconstrained version of the control strategy performs as a feedback linearization control. The results confirm that a reduction in the prediction time h leads to a decrease in both settling time and the speed of responses. However, this reduction is accompanied by an increase in torque magnitudes. The settling time for $h = 0.05$ is considerably smaller compared to the other cases at the cost of higher control inputs. The obtained results are in full alignment with the outcomes of Remark 2 in Sect. 2 for the unconstrained control. However, the computed torques for the unconstrained controller exceed admissible ranges and are unfeasible for practical realization. To decrease the applied torques, the prediction time h seems to be increased. However, it negatively affect the speed of the response. According to the results of Fig. 3, the settling time for $h = 0.4$ is high while the control input is still out of the specified range.

Consequently, the unconstrained controller with high values of h is found to be inefficient for limiting the control input and the application of the constrained controller is required. Note that, $h = 0.4$ is removed at the rest of the results because of its high settling time.

The constrained controller is evaluated in the simulation results, considering the maximum allowable torques that the actuator can apply. The results for $h = 0.05$ and 0.2 are shown in Fig. 4. Since the unconstrained controller demands larger control input for lower prediction time value ($h = 0.05$), the constrained controller often encounters more saturations. This result is in complete agrement with the result of Theorem 2. Consequently, it is crucial to choose a suitable prediction time that is neither too large nor too small. The suitable value for the simulated system can be found $h = 0.2$. The system slows down for higher values like $h = 0.4$, and the control input becomes more saturated for smaller values like $h = 0.05$. Equivalently, it is obvious that the reduction factor is changed between 0 and 1 according to Fig. 4d. When $\kappa = 1$, there is no limitation on the control signal. However, during saturation, the factor κ is decreased to reduce the control input τ.

To assess the effectiveness of the suggested constrained control approach in comparison to alternative constrained strategies, the achieved outcomes are contrasted with those of the conventional NMPC outlined in Appendix 1, considering time-varying trajectories. Both control methods
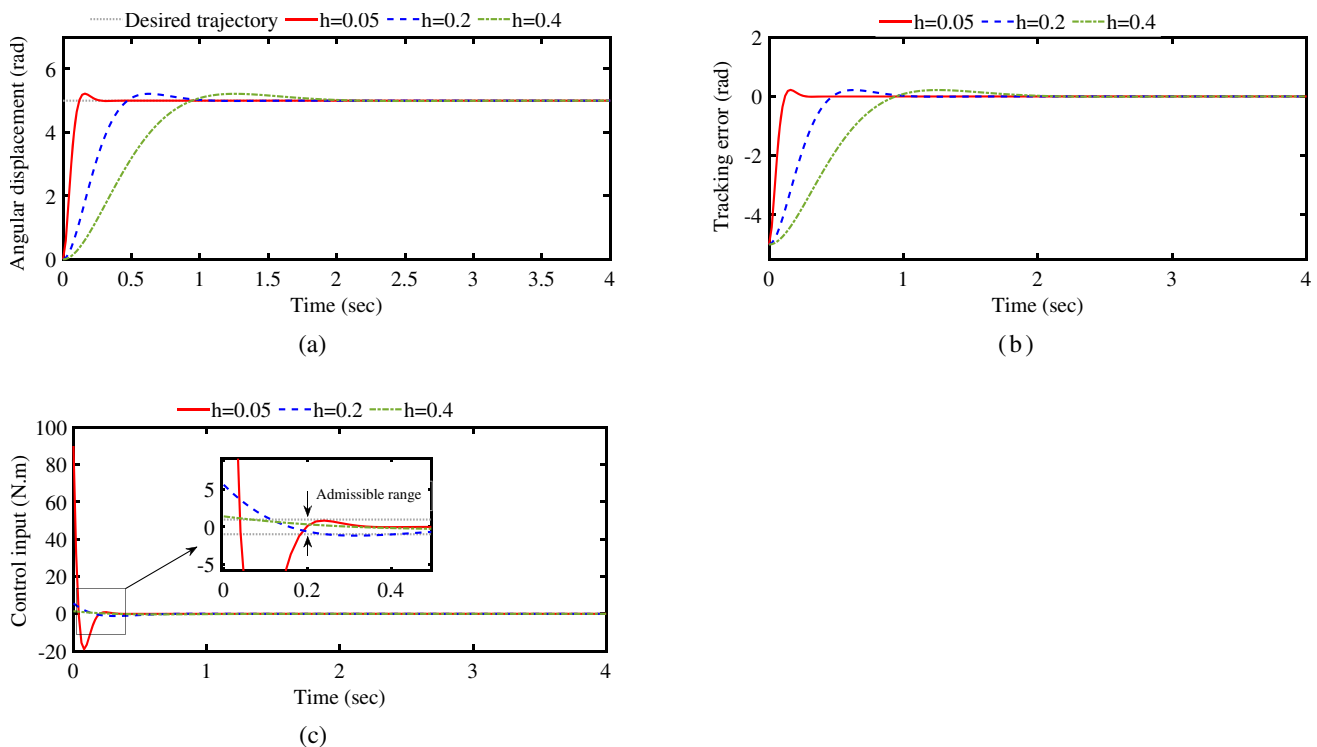

Fig. 3 The simulation results of the unconstrained control for step trajectory, a Angular displacement, b Tracking error, c Control input
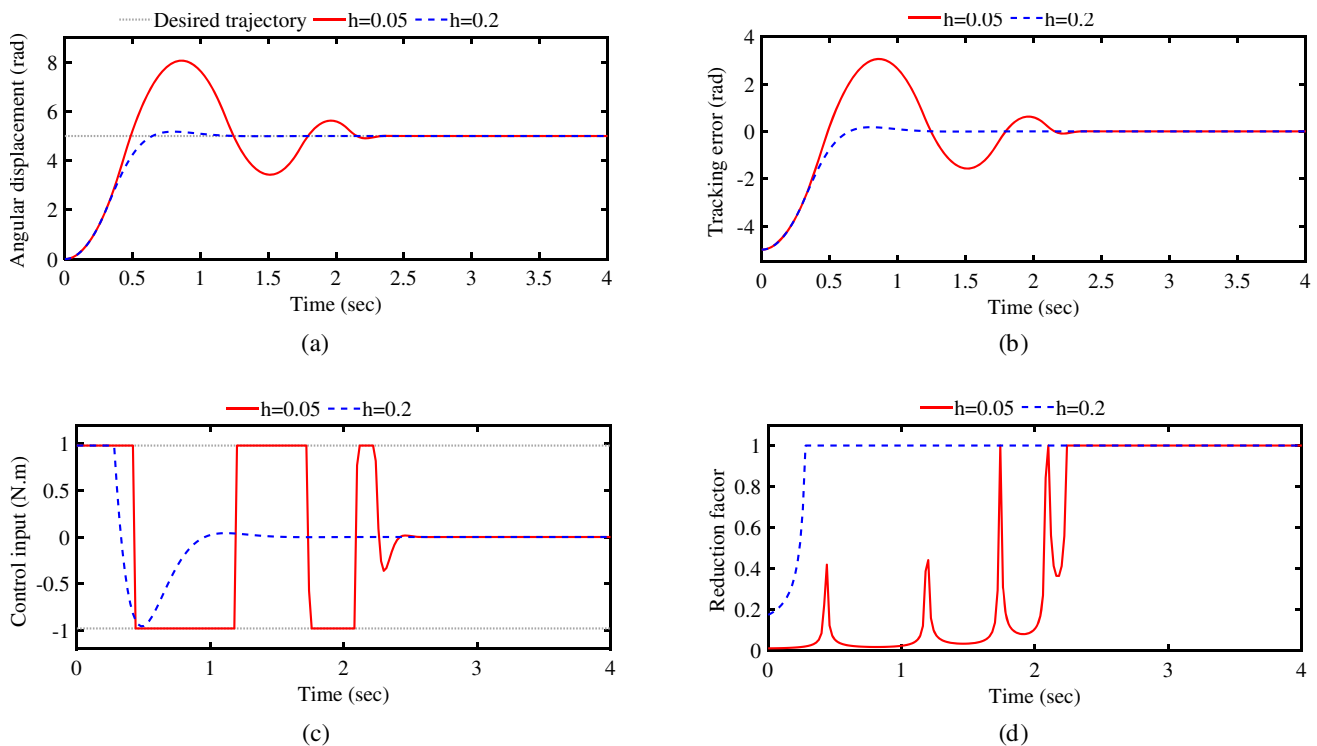
Fig. 4 The simulation results of the constrained control for step trajectory, **a** Angular displacement, **b** Tracking error, **c** Control input, **d** Reduction factor

utilize identical non-linear lever arm models and constraints. According to Fig. 5, the performance of two methods in satisfying the constraints are similar. However, the simulation times for the proposed controller and NMPC running on the same PC are 1.75 (sec) and 72.8 (sec), respectively. This result indicates that the proposed constrained controller is much faster than the NMPC. This is for the reason that the NMPC, unlike the proposed method, uses the online optimization for calculation of the control inputs at each sampling time. These comparative results indicate the capability of the proposed method for online implementation.

In order to show the independency of the proposed constrained controller on the selected value for the prediction time ($h = 0.2$), the controller is tested under the harmonic trajectories according to Fig. 6. The results indicate the superior performance of the proposed method in tracking the mentioned trajectory with admissible control inputs. Also, the simulation times are 1.73 (s) and 85.05 (s) for the proposed method and NMPC, respectively. Therefore, the proposed method is fast and easy to implement compared to the common NMPC method.

3.2 Experimental Evaluation of the Proposed Control System

To implement the proposed control system in the real environment, a platform for a lever arm is designed and fabricated. The fabricated platform containing a lever-arm with two end-point masses is shown in Fig. 7. The derive pulleys and conveyor tail connect the DC motor to the arm. The MEMS-grade MPU6050 inertial measurement unit (IMU) is employed to measure the angular velocity of the arm at a frequency of 50 Hz, as depicted in Fig. 7. Additionally, the HN3806 two-phase encoder provides the angular displacement of the arm with an accuracy of 0.3 degrees. The measured data sent to the Simulink software through the serial connection, is used to calculate the control signal. Finally, the pulse-width modulation (PWM) input is sent to a 12-volt DC motor to complete the hardware in the loop structure. In this setup, two Arduino UNO boards serve as input–output (IO) hardware, while the analysis and calculation of the control input are executed on a laptop computer equipped with an Intel(R) Core(TM) i7 CPU 6500U running at 2.50 GHz and 4 MB cache. Note that, the admissible range of the control input due to the
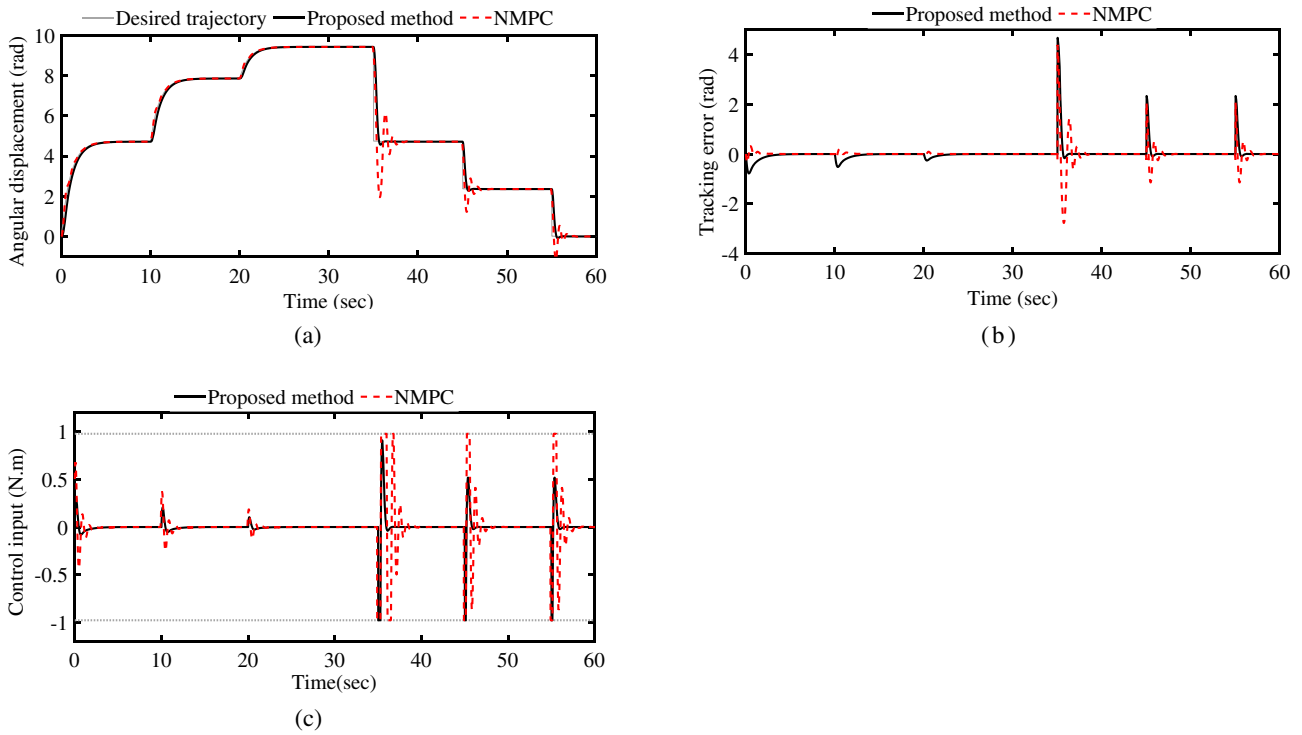
Fig. 5 The simulation results of the constrained control for time-varying trajectory in comparing with NMPC, **a** Angular displacement, **b** Tracking error, **c** Control input
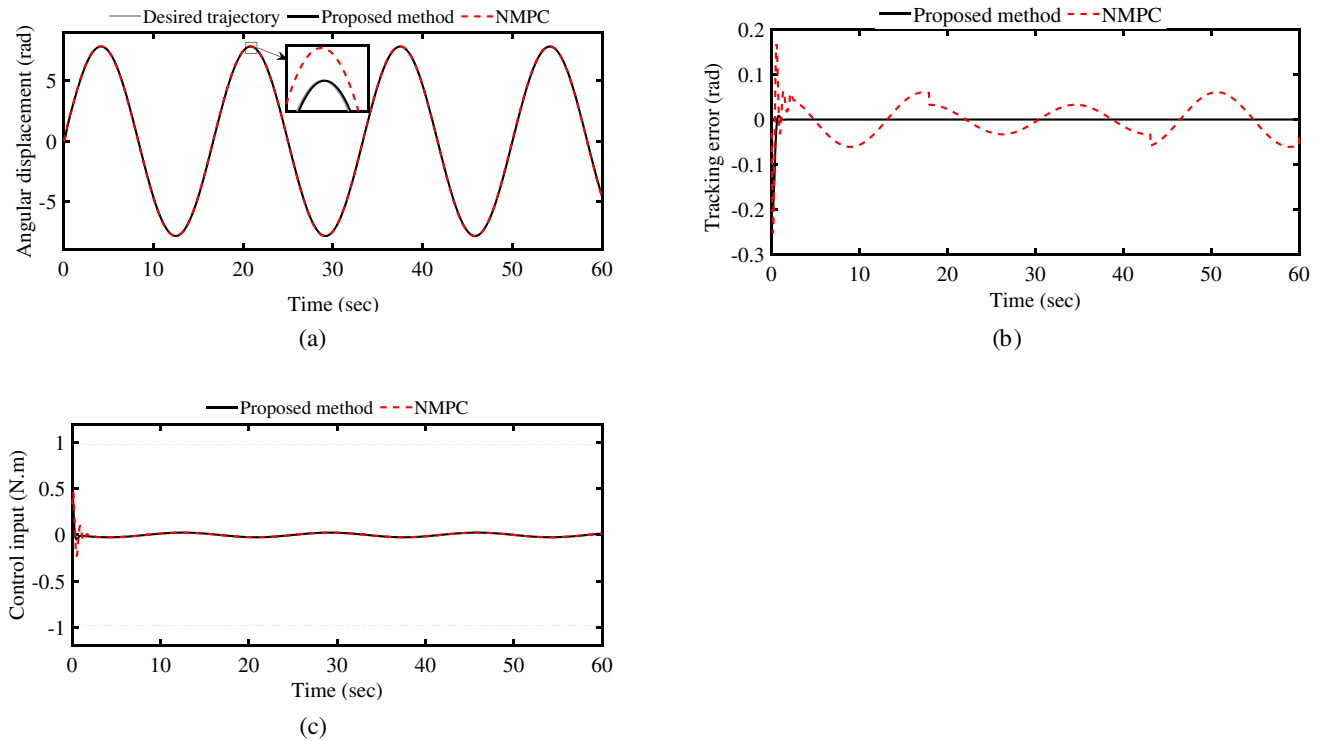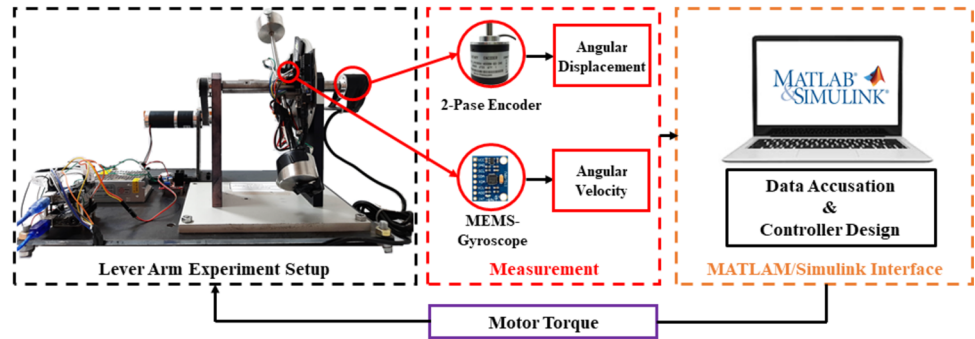

Fig. 6 The simulation results of the constrained control for harmonic trajectory in comparing with NMPC, **a** Angular displacement, **b** Tracking error, **c** Control input

Fig. 7 Experimental setup

limited capacity of actuator is considered as $-0.98 \leq \tau \leq 0.98$ (N m). On the another hand, in simulation studies, the impact of the time-delay is dropped. However in the real system, time delay from the sensor signal and control input can be clearly seen.

3.2.1 Results Without Perturbations

In this section, the results of the proposed controller are presented by assuming no external disturbances and parametric uncertainties. Additionally, the gyroscope data is incorporated in these results to provide the angular velocity of the lever-arm. Figures 8 and 9 show the obtained results of the proposed control method during two desired trajectories. The results clearly show a good performance in

tracking the desired trajectories by the proposed control method. It is necessary to say that when the reduction factor is equal to one, the control input is in the admissible range, and there is no reduction in the control input. However, the reduction factor is reduced during saturation to limit the control input τ. The NMPC algorithm used as a comparative method in the simulation studies is not applicable for the online implementation in the experimental setup because of its too high running time.

3.2.2 Results with Perturbations

In the following, the effectiveness of the proposed ESO-based constrained controller is assessed by incorporating 20% parametric uncertainty in the lever arm lengths and an
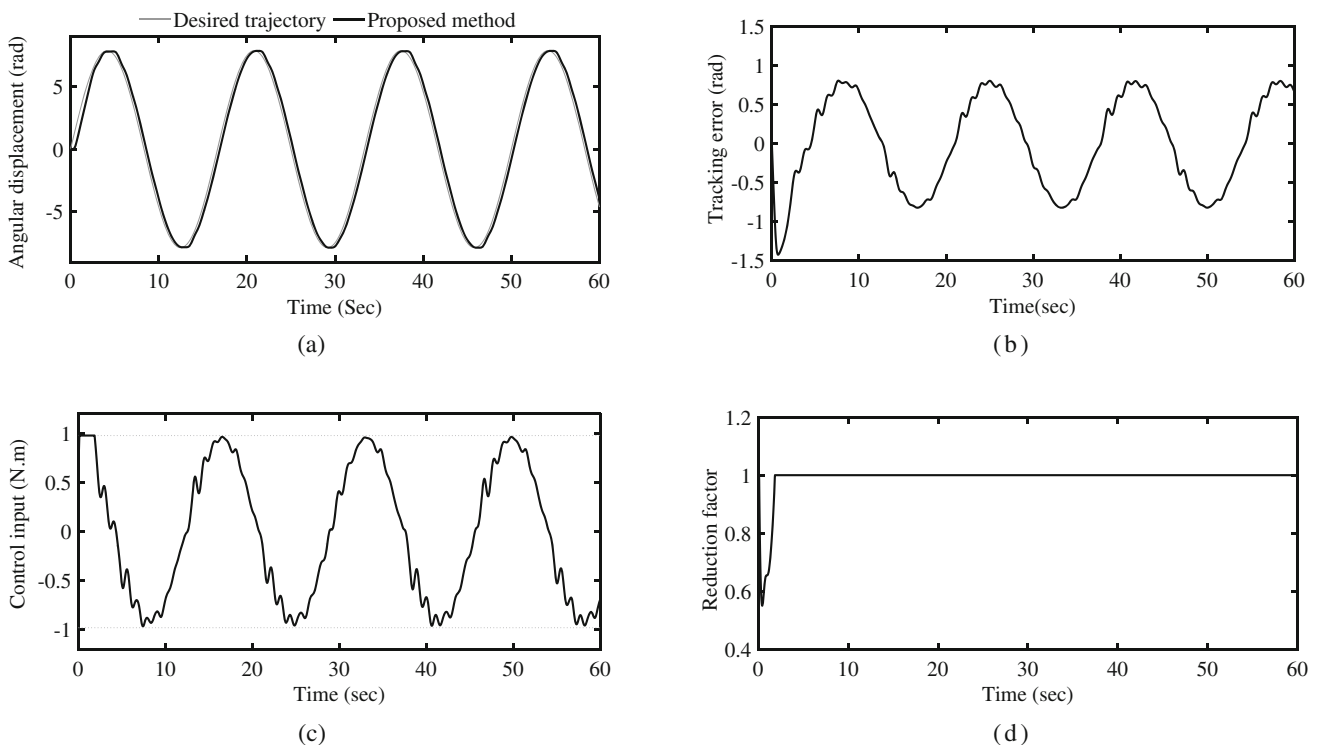

Fig. 8 The experimental results of the constrained control for the periodic path, **a** Angular displacement, **b** Tracking error, **c** Control input, **d** Reduction factor
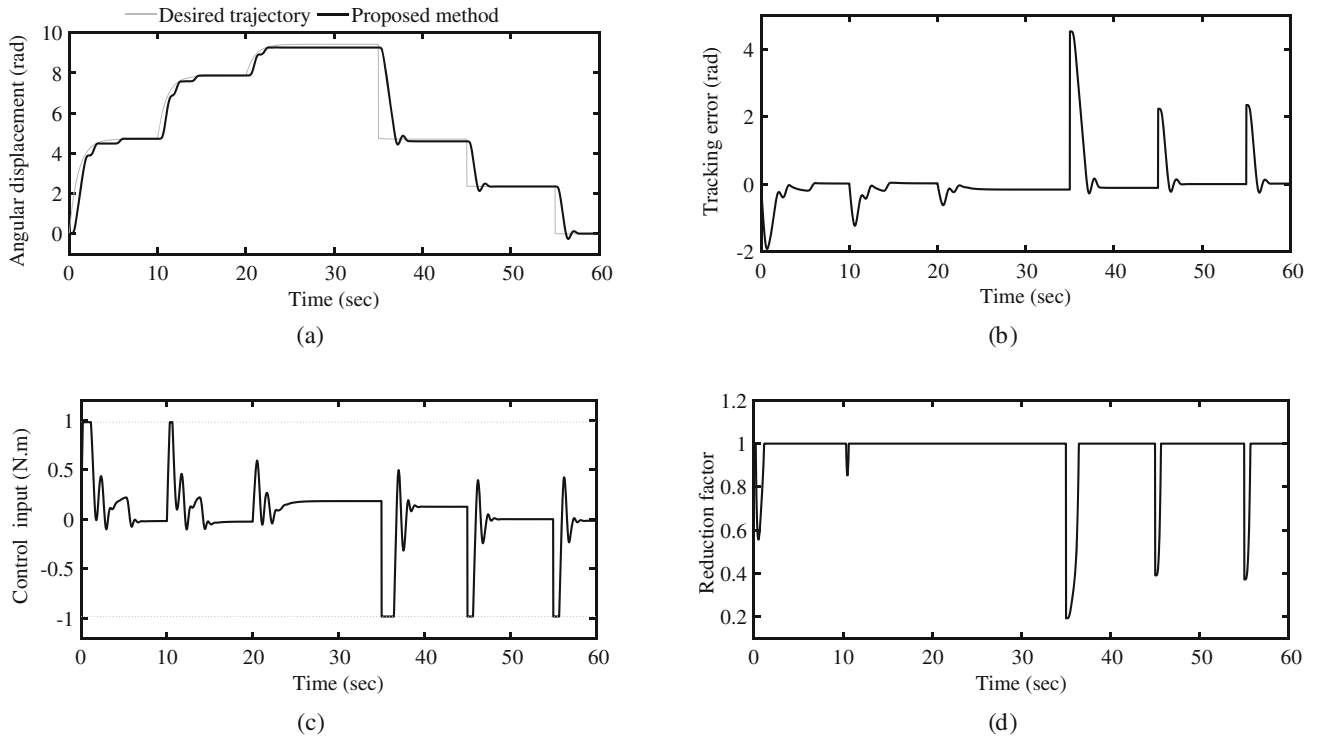
Fig. 9 The experimental results of the constrained control for time-varying path, **a** Angular displacement, **b** Tracking error, **c** Control input, **d** Reduction factor
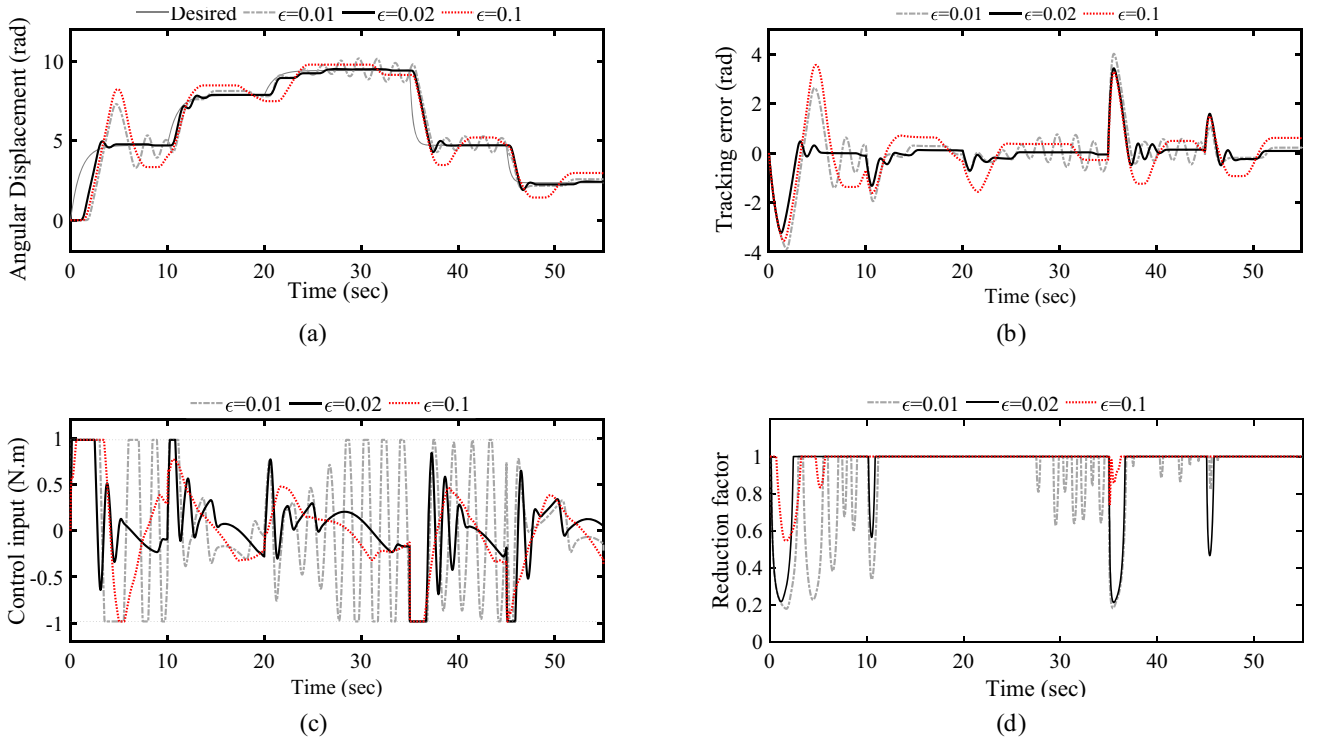

Fig. 10 The experimental results of the ESO-based controller for different ϵ, **a** Angular displacement, **b** Tracking error, **c** Control input, **d** Reduction factor

external disturbance $d = 0.3 \sin(0.5t)$. The pseudo-code of the proposed hardware in the loop mechanization is outlined in Algorithm 1. The results of the ESO-based constrained controller for three values of the free parameter ϵ in the observer are compared in Fig. 10. As illustrated in Fig. 10, for a higher value for $\epsilon = 0.1$, the controller couldn't properly follow the desired path. This shows that larger values of ϵ may not effectively provides the dynamics of lever-arm behavior. Based on Remark 4, a decrease in the free parameter ϵ leads to a substantial reduction in the estimation error; nevertheless, there is some flexibility in reducing the value of ϵ. When the value of ϵ is much smaller, as in the case of $\epsilon = 0.01$, the system becomes sensitive to modeling and measurement errors, resulting in fluctuations as illustrated in Fig. 10b. Numerical errors may also arise when employing much smaller values for the observer gain. The control inputs associated with three different values of ϵ are depicted in Fig. 10c. The outcomes shows that the fluctuations observed for $\epsilon = 0.01$ result in a more saturated control input. Therefore, ϵ should be chosen appropriately, avoiding both excessively large and excessively small to mitigate substantial errors and fluctuations in the system responses and control input. Based on the results, the choice of $\epsilon = 0.02$ is considered reasonable for the present application.

Algorithm 1 The proposed control method pseudo-code

Require Encoder data
Initialization: $t = 0$,
While $t < t_{\text{end}}$
Set Encoder data.
Set Estimates states, $\hat{x}_{i\ (i=1,2,3)}$ using Eq. (41).
Set Calculate constrained control input τ using Eq. (21).
Set Update the constrained controller by supervisor using $\hat{x}_3$
Set Transform the control input to PWM.
Set Send the obtained PWM to the DC motor.
end while

Figure 11 illustrates a comparison among the estimated states and the unknown term ($\hat{x}_3$) for three different free parameters of ϵ. It is clearly seen that, reducing the parameter ϵ until an acceptable range can reduce the estimation errors. Note that, the gyroscope data is used to calculate the estimation error of the second state $\tilde{e}_2$.

To evaluate the proposed method under various conditions, a time-varying reference trajectory is used. The outcomes are then compared with those obtained from the controller without utilizing the estimated unknown term.

Figure 12 illustrates that the ESO-based controller outperforms the controller without ESO, demonstrating significantly enhanced performance. This is attributed to the fact that the estimator tries to improve the precision of the controller by incorporating the perturbation term. Therefore, the ESO-based controller, employing the ESO, demonstrates superior performance in reducing the tracking error. In addition, the controller without ESO brings high control input to compensate for the perturbations. Therefore, the difference between the ESO-based controller and the controller without ESO is emphasized in the tracking accuracy of the reference path with lower control efforts. This is because the ESO-based method, as an adaptive control approach, utilizes perturbation information to calculate the control input at each sampling time. In contrast, the controller without ESO attempts to reduce the tracking error by increasing the control effort.

To assess the efficiency of the proposed observer-based controller in compensating for the perturbations, the obtained results are compared with those extracted by an adaptive back-stepping controller (ABSC), addressed in the Appendix. In this case, the periodic path is determined. Note that, the amplitude and frequency of the external disturbance are unknown for both controller. According to Fig. 13, the tracking error of the proposed ESO-based controller is lower than that of the ABSC. The ABSC controller couldn't estimate the perturbation term accurately, unlike the ESO. Note that the adaptive control laws like ABSC often require primary information of the unknown terms.

4 Conclusion

In this study, a nonlinear optimal controller with input constraints is analytically designed for a class of second-order systems. The optimality of the constrained solution is
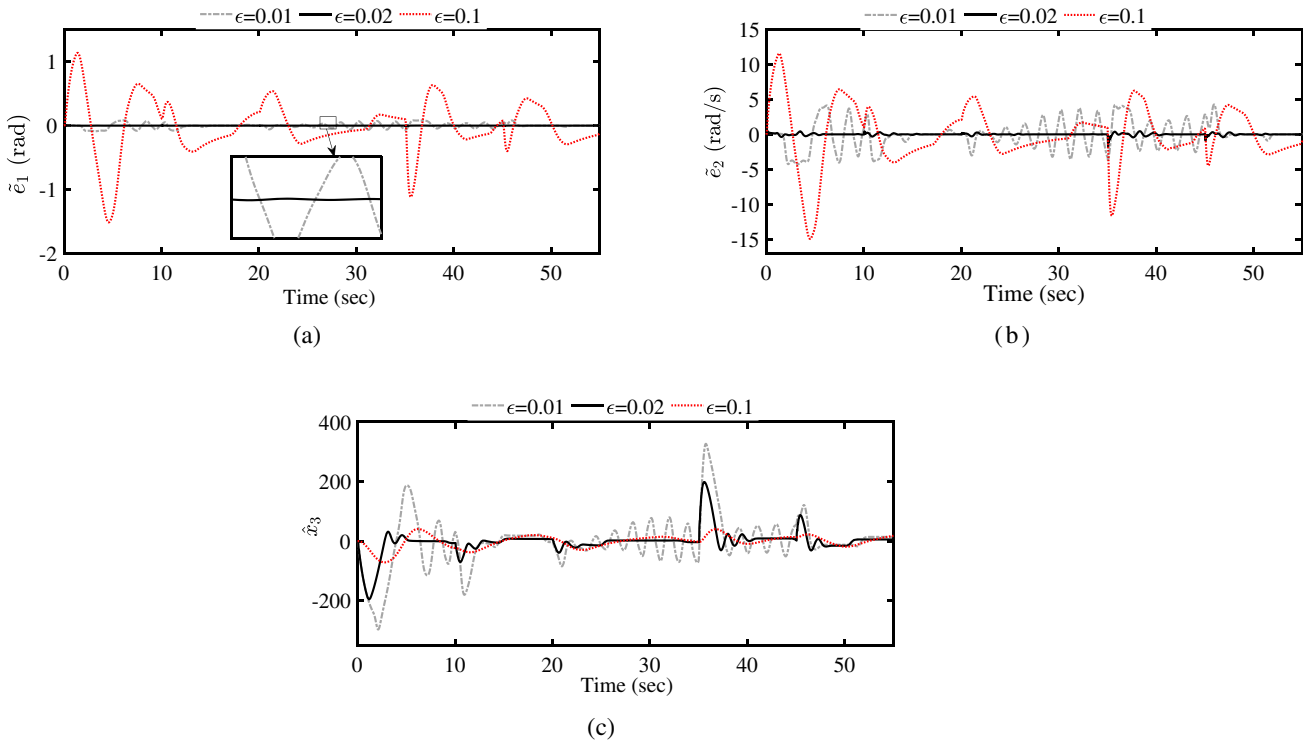
Fig. 11 The estimation results for different ϵ, **a** Angular displacement error, **b** Angular velocity error, **c** Unknown term
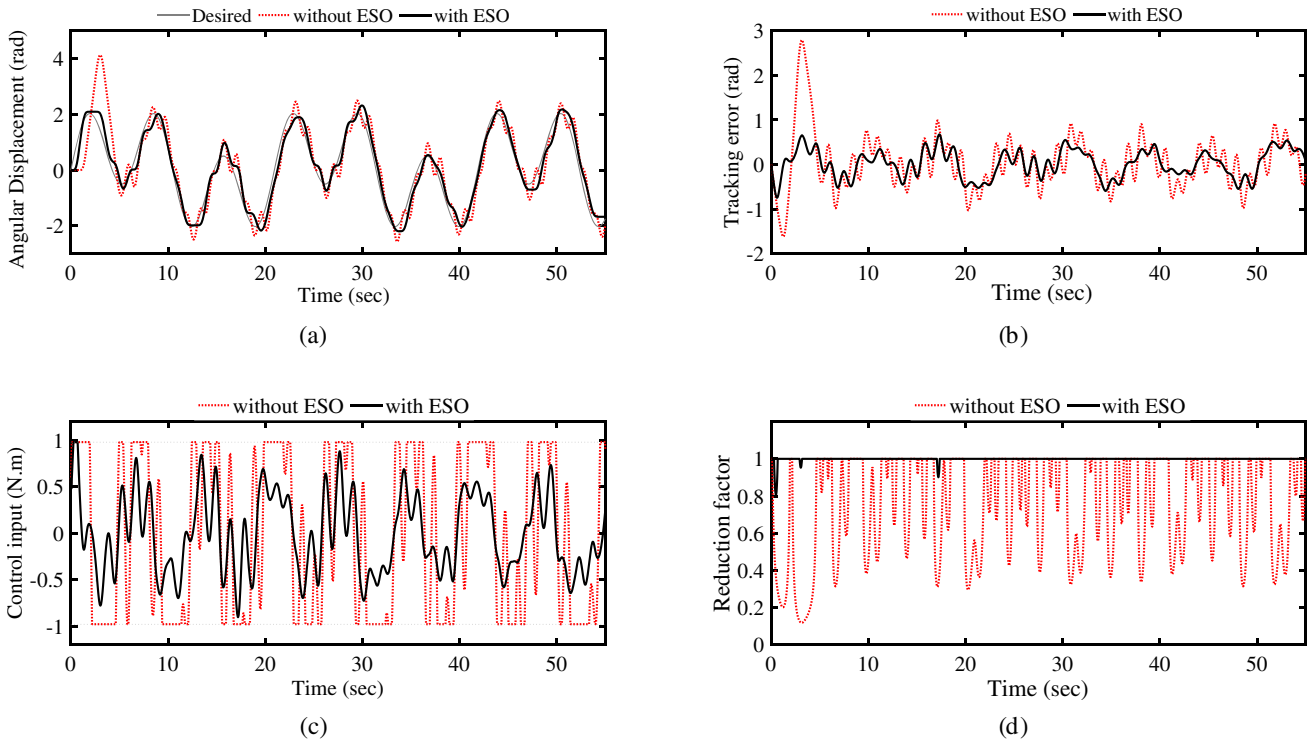

Fig. 12 The comparative experimental results of the controller with and without ESO for time-varying path, **a** Angular displacement, **b** Tracking error, **c** Control input, **d** Reduction factor
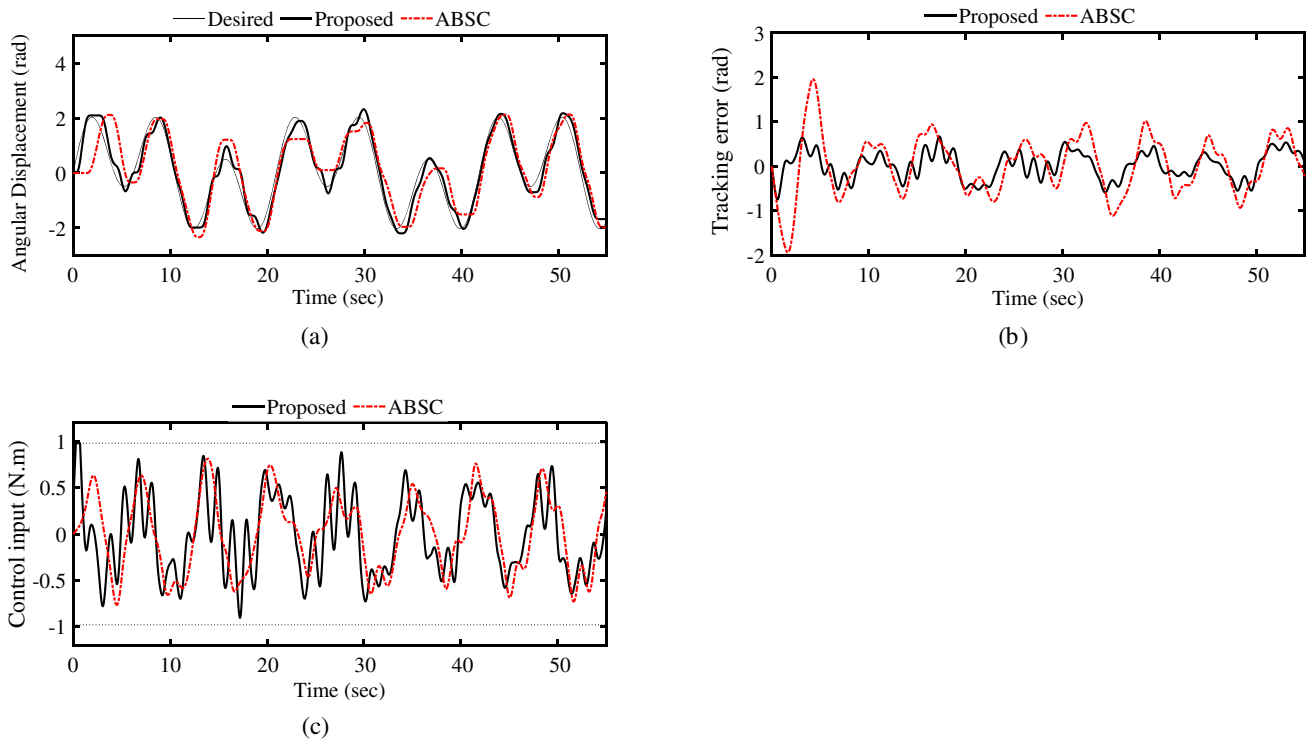
Fig. 13 The comparative experimental results between the proposed method and ABSC for the time-varying path, **a** Angular displacement, **b** Tracking error, **c** Control input

provided by solving an optimization problem based on the response prediction of nonlinear systems. The stability of the constrained controller is analyzed to show the convergence of the tracking errors towards the compact sets in terms of the prediction time. Consequently, it is essential to strike a balance when selecting the prediction time, avoiding both excessively large and excessively small values. Opting for a prediction time that is too large leads to slow responses, while choosing a prediction time that is too small results in more saturated control input, deteriorating the responses of the system. The ESO is employed to compensate for uncertainties and external disturbances, updating the proposed constrained controller to match real conditions. Simulation studies are carried out for a lever arm, and the proposed control schemes have been compared with NMPC. The results show that the proposed controller is much faster than NMPC. Therefore, it is able to be online implemented on a fabricated platform containing a lever arm. The proposed control method is verified with different tests. The results demonstrate the efficacy of the proposed control method in minimizing tracking errors in the presence of input limitations. The comparative results with the ABSC indicate superior performance for the proposed method in compensating for uncertainties and external disturbances. The extension of the proposed methodology to address more complex second-order systems with multi inputs opens avenues for future research and improvements.

Appendix 1: Nonlinear Model Predictive Control Algorithm

The nonlinear model predictive control (NMPC) is an conventional effective method to constrained control of nonlinear systems. In order to show the performance of the proposed constrained controller for the lever arm, the results are compared with a constrained NMPC. The overall structure of constrained NMPC algorithm is shown in Fig. 14. According to Fig. 14, the NMPC algorithm includes, prediction block predicts the future states, cost function block, and minimization block that minimize the cost function in the presence of state constraints. The discrete model of lever arm is used in this algorithm. According to Fig. 15, the control and predictive horizon of the NMPC algorithm is chosen 5 and 10 steps, respectively.
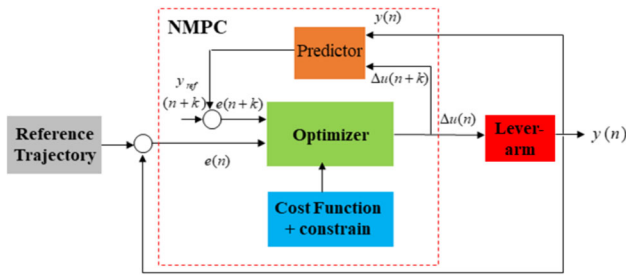
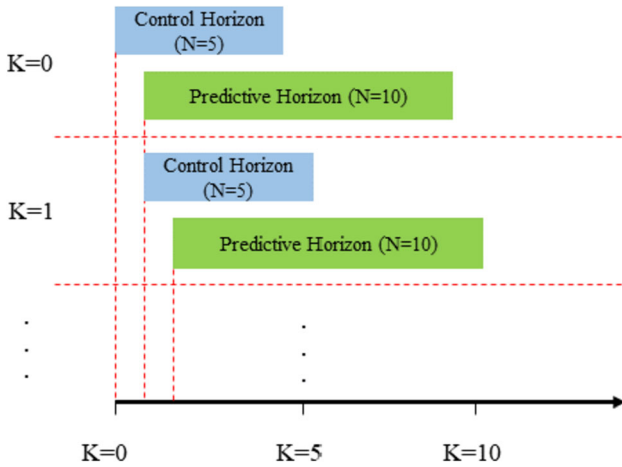Fig. 14 The overall structure of NMPC algorithm for a lever arm

Fig. 15 A discrete NMPC approach

Consequently, when $k = 0$, the control horizon will be from $k = 0$ to $k = 4$ and the predictive horizon will be from $k = 1$ to $k = 10$.

Appendix 2: Adaptive Back-stepping with Tuning Function for Strict Feedback System

An adaptive controller is formulated by combining a parameter estimator, which furnishes estimations of unknown parameters, with a control law.

$$\begin{cases} \dot{x}_1 = x_2 + \phi_1^T(x_1)\theta + \psi_1(x_1), \\ \dot{x}_2 = au + \phi_2^T(x)\theta + \psi_2(x), \end{cases} \tag{52}$$

where θ is unknown constant, ϕ_i and ψ_i, $i = 1, 2$ are known functions, $sign(a)$ is known but a is an unknown function.

Step 1 defining the change of coordinates as

$$z_1 = x_1 - x_r, \tag{53}$$

$$z_2 = x_2 - \alpha_1 - \dot{x}_r, \tag{54}$$

which α_1 is virtual control. Derivative of the tracking error z_1 is calculated as

$$\dot{z}_1 = \dot{x}_1 - \dot{x}_r = x_2 + \phi_1^T\theta + \psi_1 - \dot{x}_r$$
$$= z_2 + \alpha_1 + \phi_1^T\theta + \psi_1. \tag{55}$$

First Lyapunov function is defined as

$$V_1 = \frac{1}{2}z_1^2 + \frac{1}{2}\tilde{\theta}^T\Gamma^{-1}\tilde{\theta}, \tag{56}$$

where $\tilde{\theta} = \theta - \hat{\theta}$ and Γ is an arbitrary positive definite matrix.

$$\dot{V}_1 = z_1\dot{z}_1 - \tilde{\theta}^T\Gamma^{-1}\dot{\hat{\theta}}. \tag{57}$$

Substituting (55) in (57)

$$\dot{V}_1 = z_1\left(z_2 + \alpha_1 + \phi_1^T\hat{\theta} + \psi_1\right) - \tilde{\theta}^T\Gamma^{-1}\dot{\hat{\theta}}. \tag{58}$$

Choosing $\dot{\hat{\theta}} = \Gamma\phi_1 z_1$ and $\alpha_1 = -c_1 z_1 - \phi_1^T\hat{\theta} - \psi_1$ leads to $\dot{V}_1 \leq 0$, where c_1 and $\hat{\theta}$ are a positive constant and an estimate of θ, respectively.

Considering $\tau_1 = \Gamma\phi_1 z_1$ as first tuning function, first derivative of Lyapunov function is rewritten as

$$\dot{V}_1 = z_1 z_2 - c_1 z_1^2 - \tilde{\theta}^T\Gamma^{-1}\left(\dot{\hat{\theta}} - \tau_1\right). \tag{59}$$

Step 2 Derivative of the second tracking error z_2 is calculated as

$$\dot{z}_2 = \dot{x}_2 - \dot{\alpha}_1 - \ddot{x}_r$$
$$= au + \phi_2^T\theta + \psi_2 - \frac{\partial\alpha_1}{\partial x_1}(x_2 + \psi_1)$$
$$- \frac{\partial\alpha_1}{\partial x_1}\phi_1^T\theta - \frac{\partial\alpha_1}{\partial\hat{\theta}}\dot{\hat{\theta}} - \ddot{x}_r. \tag{60}$$

Second lyapunov function is proposed as

$$V_2 = V_1 + \frac{1}{2}z_2^2 + \frac{|a|}{\gamma}\tilde{p}^2 \tag{61}$$

where $\tilde{p} = p - \hat{p}$ and $p = \frac{1}{a}$ and γ is a constant value. First derivative of this Lyapunov function is written as

$$\dot{V}_2 = \dot{V}_1 + z_2\dot{z}_2 - \frac{|a|}{\gamma}\tilde{p}\dot{\hat{p}}$$
$$= z_1 z_2 - c_1 z_1^2 - \tilde{\theta}^T\Gamma^{-1}\left(\dot{\hat{\theta}} - \tau_1\right)$$
$$+ z_2\left(au + \phi_2^T\theta + \psi_2 - \frac{\partial\alpha_1}{\partial x_1}(x_2 + \psi_1) - \frac{\partial\alpha_1}{\partial x_1}\phi_1^T\theta - \frac{\partial\alpha_1}{\partial\hat{\theta}}\dot{\hat{\theta}} - \ddot{x}_r\right)$$
$$+ \tilde{\theta}^T\Gamma^{-1}(\tau_1 - \dot{\hat{\theta}}). \tag{62}$$

The aim is to make $\dot{V}_2 \leq 0$. The stabilizing function α_2 is selected as

$$\alpha_2 = -c_2 z_2 - z_1 - \psi_2 + \frac{\partial \alpha_1}{\partial x_1}(x_2 + \psi_1)$$
$$- \left(\phi_2 - \frac{\partial \alpha_1}{\partial x_1}\phi_1\right)\hat{\theta} \tag{63}$$
$$+ \frac{\partial \alpha_1}{\partial \hat{\theta}}\tau_2,$$

where τ_2 is second tuning function. It is determined as below

$$\tau_2 = \tau_1 + \Gamma\left(\phi_2 - \frac{\partial \alpha_1}{\partial x_1}\phi_1\right)z_2. \tag{64}$$

First derivative of error variable can be rewritten as

$$\dot{z}_2 = -c_2 z_2 - z_1 + \left(\phi_2 - \frac{\partial \alpha_1}{\partial x_1}\phi_1\right)^T \tilde{\theta}$$
$$+ \frac{\partial \alpha_1}{\partial \hat{\theta}}\left(\tau_2 - \dot{\hat{\theta}}\right) - a\tilde{p}\bar{u}. \tag{65}$$

Substituting (65) in (62) is resulted in

$$\dot{V}_2 = -c_1 z_1^2 - c_2 z_2^2 + \tilde{\theta}^T \Gamma^{-1}\left(\tau_2 - \dot{\hat{\theta}}\right)$$
$$- \frac{|a|}{\gamma}\left(\gamma \, sign(a)\bar{u}z_2 + \dot{\hat{p}}\right) \tag{66}$$

Considering

$$u = \hat{p}\bar{u}, \quad \bar{u} = \alpha_2 + \ddot{x}_r \tag{67}$$

$$\dot{\hat{\theta}} = \tau_2 \tag{68}$$

$$\dot{\hat{p}} = -\gamma \, sign(a)\bar{u}z_2, \tag{69}$$

lead to $\dot{V}_2 \le 0$.

Declarations

Conflict of interest The authors confirm no conflict of interest in the research study made and its publishing.

References

Abdi B, Mirzaei M, Mojed Gharamaleki R (2018) A new approach to optimal control of nonlinear vehicle suspension system with input constraint. J Vib Control 24(15):3307–3320. https://doi.org/10.1177/1077546317704598

Bartolini G, Ferrara A, Usai E (1997) Output tracking control of uncertain nonlinear second-order systems. Automatica 33(12):2203–2212. https://doi.org/10.1016/S0005-1098(97)00147-7

Chen CT (1984) Linear system theory and design. Saunders college publishing, Philadelphia

Colombo L, Corradini ML, Ippoliti G, Orlando G (2020) Pitch angle control of a wind turbine operating above the rated wind speed: A sliding mode control approach. ISA Trans 96:95–102. https://doi.org/10.1016/j.isatra.2019.07.002

Cruz-Ortiz D, Chairez I, Poznyak A (2022) Non-singular terminal sliding-mode control for a manipulator robot using a barrier Lyapunov function. ISA Trans 121:268–283. https://doi.org/10.1016/j.isatra.2021.04.001

Ding S, Zheng WX (2016) Nonsingular terminal sliding mode control of nonlinear second-order systems with input saturation. Int J Robust Nonlinear Control 26(9):1857–1872. https://doi.org/10.1002/rnc.3381

Ghiasi AR, Alizadeh G, Mirzaei M (2010) Simultaneous design of optimal gait pattern and controller for a bipedal robot. Multibody Syst Dyn 23(4):401–429. https://doi.org/10.1007/s11044-009-9185-z

Gui H, Jin L, Xu S (2015) Simple finite-time attitude stabilization laws for rigid spacecraft with bounded inputs. Aerosp Sci Technol 42:176–186. https://doi.org/10.1016/j.ast.2015.01.020

He D, Li Y, Meng X, Si Q (2022) Anti-slip control for unmanned underwater tracked bulldozer based on active disturbance rejection control. Mechatronics 84:102803. https://doi.org/10.1016/j.mechatronics.2022.102803

Homayounzade M, Keshmiri M (2011) Velocity observer based controller design for second order systems, with application to constrained robotic systems. In: 2011 IEEE/ASME international conference on advanced intelligent mechatronics (AIM). IEEE, pp 588–593

Hu J, Wang P, Xu C, Zhou H, Yao J (2022) High accuracy adaptive motion control for a robotic manipulator with model uncertainties based on multilayer neural network. Asian J Control 24(3):1503–1514. https://doi.org/10.1002/asjc.2546

Jafari M, Mirzaei M, Mirzaeinejad H (2015) Optimal nonlinear control of vehicle braking torques to generate practical stabilizing yaw moments. Int J Automot Mech Eng 11(1):2639–2653. https://doi.org/10.15282/ijame.11.2015.41.0222

Jiang B, Chen H, Li B, Zhang X (2022) Sub-fixed-time control for a class of second order system. Trans Inst Meas Control 44(1):76–87. https://doi.org/10.1177/0142331220921008

Jimenez-Rodriguez E, Sanchez-Torres JD, Gomez-Gutierrez D, Loukinanov AG (2019) Variable structure predefined-time stabilization of second-order systems. Asian J Control 21(3):1179–1188. https://doi.org/10.1002/asjc.1785

Khalil H (2001) Nonlinear systems. Prentice-Hall, New Jersey

Kirk DE (2004) Optimal Control Theory (An Introduction). Dover Publications, INC, New York

Li T, Zhang S, Yang H, Zhang Y, Zhang L (2014) Robust missile longitudinal autopilot design based on equivalent-input-disturbance and generalized extended state observer approach. Proc Inst Mech Eng Part G J Aerosp Eng 229(6):1025–1042. https://doi.org/10.1177/0954410014543715

Li DP, Li DJ, Liu YJ, Tong S, Chen CP (2017) Approximation-based adaptive neural tracking control of nonlinear MIMO unknown time-varying delay systems with full state constraints. IEEE Trans Cybern 47(10):3100–3109. https://doi.org/10.1109/TCYB.2017.2707178

Li J, Ji L, Li H (2021) Optimal consensus control for unknown second-order multi-agent systems: using model-free reinforcement learning method. Appl Math Comput 410:126451. https://doi.org/10.1016/j.amc.2021.126451

Li B, Yang X, Zhou R, Wen G (2022) Reinforcement learning-based optimised control for a class of second-order nonlinear dynamic systems. Int J Syst Sci 53(15):1–11. https://doi.org/10.1080/00207721.2022.2074568

Liu D, Wang D, Yang X (2013) An iterative adaptive dynamic programming algorithm for optimal control of unknown discrete-time nonlinear systems with constrained inputs. Inf Sci 220:331–342. https://doi.org/10.1016/j.ins.2012.07.006

Loxton RC, Teo KL, Rehbock V, Yiu KFC (2009) Optimal control problems with a continuous inequality constraint on the state and the control. Automatica 45(10):2250–2257. https://doi.org/10.1016/j.automatica.2009.05.029

Lu P (1995) Optimal predictive control of continuous nonlinear systems. Int J Control 62(3):633–649. https://doi.org/10.1080/00207179508921561

Ma Z, Huang P (2020) Adaptive neural-network controller for an uncertain rigid manipulator with input saturation and full-order state constraint. IEEE Trans Cybern 52(5):2907–2915. https://doi.org/10.1109/TCYB.2020.3022084

Malekshahi A, Mirzaei M (2012) Designing a non-linear tracking controller for vehicle active suspension systems using an optimization process. Int J Automot Technol 13(2):263–271. https://doi.org/10.1007/s12239-012-0023-6

Marzban HR, Razzaghi M (2010) Rationalized Haar approach for nonlinear constrained optimal control problems. Appl Math Model 34(1):174–183. https://doi.org/10.1016/j.apm.2009.03.036

Mashayekhi S, Ordokhani Y, Razzaghi M (2012) Hybrid functions approach for nonlinear constrained optimal control problems. Commun Nonlinear Sci Numer Simul 17(4):1831–1843. https://doi.org/10.1016/j.cnsns.2011.09.008

Miranda-Colorado R (2019) Finite-time sliding mode controller for perturbed second-order systems. ISA Trans 95:82–92. https://doi.org/10.1016/j.isatra.2019.05.026

Mirzaeinejad H, Mirzaei M (2011) A new approach for modelling and control of two-wheel anti-lock brake systems. Proc Inst Mech Eng Part K J Multi-body Dyn 225(2):179–192. https://doi.org/10.1177/2041306810394937

Mirzaeinejad H, Mirzaei M, Kazemi R (2016) Enhancement of vehicle braking performance on split-μ roads using optimal integrated control of steering and braking systems. Proc Inst Mech Eng Part K J Multi-body Dyn 230(40):401–415. https://doi.org/10.1177/1464419315617332

Moradi Nerbin M, Mojed Gharamaleki R, Mirzaei M (2017) Novel optimal control of semi-active suspension considering a hysteresis model for MR damper. Trans Inst Meas Control 39(5):698–705. https://doi.org/10.1177/0142331215618446

Nguyen VC, Vo AT, Kang HJ (2020) A non-singular fast terminal sliding mode control based on third-order sliding mode observer for a class of second-order uncertain nonlinear systems and its application to robot manipulators. IEEE Access 8:78109–78120. https://doi.org/10.1109/ACCESS.2020.2989613

Rafatnia S, Mirzaei M (2022) Estimation of reliable vehicle dynamic model using IMU/GNSS data fusion for stability controller design. Mech Syst Signal Proc 168:108593. https://doi.org/10.1016/j.ymssp.2021.108593

Rafatnia S, Mirzaei M (2022) Adaptive estimation of vehicle velocity from updated dynamic model for control of anti-lock braking system. IEEE Trans Intell Transp Syst 23(6):5871–5880. https://doi.org/10.1109/TITS.2021.3060970

Rao SS (2019) Engineering optimization: theory and practice. John Wiley Sons, Hoboken

Razmjooei H, Shafiei MH, Palli G, Arefi MM (2022) Nonlinear finite-time tracking control of uncertain robotic manipulators using time-varying disturbance observer-based sliding mode method. J Intell Robot Syst 104(2):36. https://doi.org/10.1007/s10846-022-01571-x

Silva NF Jr, Dórea CET, Maitelli AL (2019) An iterative model predictive control algorithm for constrained nonlinear systems. Asian J Control 21(5):2193–2207. https://doi.org/10.1002/asjc.1815

Su Y, Swevers J (2014) Finite-time tracking control for robot manipulators with actuator saturation. Robot Comput-Integr Manuf 30(2):91–98. https://doi.org/10.1016/j.rcim.2013.09.005

Tsai JH, Du YY, Zhuang WZ, Guo SM, Chen CW, Shieh LS (2011) Optimal anti-windup digital redesign of multi-input multi-output control systems under input constraints. IET Control Theory Appl 5(3):447–464. https://doi.org/10.1049/iet-cta.2010.0020

Wen GX, Chen CP, Liu YJ, Liu Z (2015) Neural-network-based adaptive leader-following consensus control for second-order non-linear multi-agent systems. IET Control Theory Appl 9(13):1927–1934. https://doi.org/10.1049/iet-cta.2014.1319

Xiong S, Wang W, Liu X, Chen Z, Wang S (2015) A novel extended state observer. ISA Trans 58:309–317. https://doi.org/10.1016/j.isatra.2015.07.012

Yi S, Zhai J (2019) Adaptive second-order fast nonsingular terminal sliding mode control for robotic manipulators. ISA Trans 90:41–51. https://doi.org/10.1016/j.isatra.2018.12.046

Yue M, Liu B, An C, Sun X (2014) Extended state observer-based adaptive hierarchical sliding mode control for longitudinal movement of a spherical robot. Nonlinear Dyn 78(2):1233–1244. https://doi.org/10.1007/s11071-014-1511-1